OPEN ACCESS Freely available online

PLOS | ONE

Prevalence of Dural Ectasia in Loeys-Dietz Syndrome: Comparison with Marfan Syndrome and Normal Controls

Atsushi K. Kono[1]*, Masahiro Higashi[2], Hiroko Morisaki[3], Takayuki Morisaki[3], Hiroaki Naito[2], Kazuro Sugimura[1]

1 Department of Radiology, Kobe University Graduate School of Medicine, Kobe Japan, **2** Department of Radiology, National Cardiovascular Research Center, Suita, Japan, **3** Department of Bioscience, National Cardiovascular Research Center, Suita, Japan

Abstract

Background and Purpose: Dural ectasia is well recognized in Marfan syndrome (MFS) as one of the major diagnostic criteria, but the exact prevalence of dural ectasia is still unknown in Loeys–Dietz syndrome (LDS), which is a recently discovered connective tissue disease. In this study, we evaluated the prevalence of dural ectasia in LDS according by using qualitative and quantitative methods and compared our findings with those for with MFS and normal controls.

Material and Methods: We retrospectively studied 10 LDS (6 males, 4 females, mean age 36.3 years) and 20 MFS cases (12 males, 8 females, mean age 37.1 years) and 20 controls (12 males, 8 females, mean age 36.1 years) both qualitatively and quantitatively using axial CT images and sagittal multi-planar reconstruction images of the lumbosacral region. For quantitative examination, we adopted two methods: method-1 (anteroposterior dural diameter of S1> L4) and method-2 (ratio of anteroposterior dural diameter/vertebral body diameter>cutoff values). The prevalence of dural ectasia among groups was compared by using Fisher's exact test and the Tukey–Kramer test.

Results: In LDS patients, the qualitative method showed 40% of dural ectasia, the quantitative method-1 50%, and the method-2 70%. In MFS patients, the corresponding prevalences were 50%, 75%, and 85%, and in controls, 0%, 0%, and 5%. Both LDS and MFS had a significantly wider dura than controls.

Conclusions: While the prevalence of dural ectasia varied depending on differences in qualitative and quantitative methods, LDS as well as MFS, showed, regardless of method, a higher prevalence of dural ectasia than controls. This finding should help the differentiation of LDS from controls.

Citation: Kono AK, Higashi M, Morisaki H, Morisaki T, Naito H, et al. (2013) Prevalence of Dural Ectasia in Loeys-Dietz Syndrome: Comparison with Marfan Syndrome and Normal Controls. PLoS ONE 8(9): e75264. doi:10.1371/journal.pone.0075264

Editor: Bart Dermaut, Pasteur Institute of Lille, France

Received April 17, 2013; **Accepted** August 12, 2013; **Published** September 25, 2013

Funding: Dr Hiroko Morisaki received a Health Labour Sciences Research Grant (Research on Measures for Intractable Diseases) from the Ministry of Health, Labour and Welfare. The funders had no role in study design, data collection and analysis, decision to publish, or preparation of the manuscript.

Competing Interests: The authors have declared that no competing interests exist.

* E-mail: akono@med.kobe-u.ac.jp

Introduction

Loeys–Dietz syndrome (LDS) is a newly discovered connective tissue disease caused by mutations in the gene of transforming growth factor β receptor (TGFBR) -1 or -2 [1,2]. The cardinal features of LDS consist of craniofacial features characterized by widely spaced eyes (orbital hypertelorism), bifid uvula and/or cleft palate, and cardiovascular diseases such as aortic root dilatation or aortic dissection, arterial tortuosity and aneurysms [2,3]. LDS shares many of its clinical features with Marfan syndrome (MFS) [4], which is an autosomal dominant connective tissue disorder caused by mutations in the gene of fibrillin-1 (FBN-1) [5]. The main features of MFS occur in skeletal, ocular, and cardiovascular areas, but other organs can also be affected, including skin, lung, and dura [6].

While LDS and MFS show striking pleiotropism and clinical variability, no clinical criteria for LDS have as yet been established in contrast to MFS, for which detailed diagnostic criteria have been developed [6,7]. The old 'Ghent nosology' for MFS classifies the clinical manifestations into major and minor criteria [6]. Dural ectasia (DE), which is also observed in neurofibromatosis type 1 and Ehlers–Danlos syndrome [6,8], is, after aortic dilatation/dissection, the second most common major criterion for MFS [8,9]. In the revised Ghent nosology, DE is no longer a critical criterion for MFS. As the finding of DE is used for the scoring of systemic features when the patients show aortic diseases, but do not have the ectopia lentis, the importance of DE remains in the new criteria. While the importance of DE is well recognized in MFS, only a few reports have dealt with the prevalence of DE in LDS [1,10,11]. DE usually occurs in connective tissues diseases, and occurs in the lumbar or sacral spine due to gravity. DE is characterized by widening of the spinal canal, posterior scalloping of the vertebral body, increased thinning of the cortex of pedicles and laminae, widening of the neural foramina or the presence of a meningocele [6]. While at present there is no standardized method for the diagnosis of DE, some qualitative [6,8] and quantitative methods [9,12,13] have been reported.

To establish clinical diagnostic criteria for LDS, the prevalence of DE has to be analyzed. In this study, we used qualitative and

quantitative methods to evaluate the prevalence of DE in LDS in comparison with that in MFS and controls.

Materials and Methods

The institutional review board (National Cardiovascular Research Center, Japan) approved this retrospective case-controlled study and written informed consent to analyze clinical data and gene mutations was obtained from all LDS and MFS subjects. In addition, written informed consent for the CT examinations was obtained from all subjects. The institutional review board waived written informed consent from the normal controls because this was a retrospective study.

Patient Population

The CT data in our institutional database was reviewed from June 2007 to July 2010. Ten LDS patients with an identified mutation in TGFBR (6 males, 4 females, mean age 36.3 years, range 20−54 years) were retrospectively reviewed from our institutional database which comprised about 20 LDS patients. These 10 patients had undergone CT examination in the lower abdominal and pelvic regions and were consecutively enrolled. Nine of them (90%) were in the post-operative stage (1 with aortic repair, 3 with valve replacement, and 5 with both). Reasons for hospitalization were aortic root dilatation in 4 patients and aortic dissection in 6 patients. Gene analysis showed 4 mutations in TGFBR-1 and 6 in TGFBR-2.

Twenty MFS patients with an identified mutation in FBN-1 (12 males, 8 females, mean age 37.1 years, range 20−56 years) were also reviewed. MFS patients who were matched to LDS patients in gender and age were randomly selected from our database, which comprises more than 100 MFS patients with mutation in FBN-1. Seventeen of the enrolled patients (85%) were in the post-operative stage (3 with aortic repair, 7 with valve replacement, and 7 with both). Reasons for hospitalization were aortic root dilatation in 11 patients, aortic dissection in 8 patients, and mitral valve regurgitation in 1 patient.

All LDS and MFS patients underwent clinical examinations including a physical examination and laboratory tests by a cardiovascular team. Initial and follow up CT examinations were performed in a clinical setting as described below. Genetic analysis was performed for all patients in the same manner as previously reported [11].

Twenty control subjects (12 males, 8 females, mean age 36.1 years, range 22−52 years) who were matched to LDS patients in gender and age were also randomly selected from our CT database. These subjects did not meet any of the major nor minor criteria of Ghent nosology. No gene analysis was performed for this group.

MFS patients and control subjects were matched to LDS in gender and age to avoid the need for adjusting the values of variables after they had been measured.

Imaging and Measurements

All LDS and MFS patients underwent CT examination (including CT angiography) using 16- or 64-MSCT at initial diagnosis or clinical follow-up for evaluation of the vascular tree. The CT covered the area from the thorax to the pelvis. Control subjects underwent CT examination covering the lower abdominal and pelvic regions as indicated by clinical need. Axial CT images with 2 mm slice thickness were obtained from all subjects and used to reconstruct multi-planar reconstruction (MPR) images. All images were transferred to CT image server and could be read on a PACS (Picture Archiving and Communication System) viewer. Two radiologists (A.K.K. and M.H. with 9 and 19 years experience, respectively, in diagnostic radiology) reviewed the CT images (qualitative inspection, described below) blinded to the genetic diagnosis. And one of the two radiologists (A.K.K.) evaluated CT images using the two quantitative methods described below.

Qualitative Inspection

DE is defined as widening of the spinal canal, posterior scalloping of the vertebral body, increased thinning of the cortex of pedicles and laminae, widening of the neural foramina or the presence of a meningocele [8,14,15]. The presence of an anterior sacral meningocele was diagnosed when herniation of the dural sac resulting from a defect in the anterior surface of the sacrum was seen [16]. Presence of a lateral meningocele was diagnosed when the nerve root sleeve was wide throughout the intervertebral foramen and ended in a pouch [17].

Quantitative Inspection

Method-1 proposed by Ahn et al. [9] (Fig. 1). Dural sac diameter (DSD) was measured in the mid-sagittal plane of the MPR image from the lumbus through to the sacrum. DE is diagnosed when the sagittal anteroposterior diameter of the spinal canal at S1 or below is greater than that at the mid axis of L4.

$$DE = DSD(S) > DSD(L4)$$

Method-2 proposed by Oosterhof et al. [12] (Fig. 1). The vertebral body diameter (VBD) and DSD were measured perpendicular to the long axis of the dural sac and vertebral body. VBD and DSD values were obtained at the midcorpus level of L1 to S1. The dural sac ratio (DSR) was calculated at L1 to S1 by dividing DSD by VBD. DE is considered present if DSR exceeds the cutoff value, which is defined as mean+2 SD of controls.

$$DSR = DSD/VBD$$

$$DE = DSR > \text{cutoff value at any level}$$

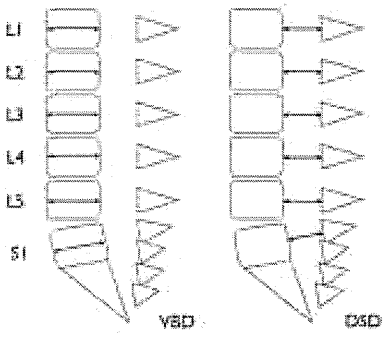

Figure 1. Scheme of sagittal CT images of the lumbosacral spine. Lines with arrows represent measurements of vertebral body diameters (VBD) and dural sac diameters (DSD).
doi:10.1371/journal.pone.0075264.g001

Statistical Analysis

For the statistical analysis, JMP software (version 8.0, SAS Institute Inc., CA, USA) was used. Continuous data were expressed as mean±SD.

We evaluated and compared the prevalence of DE in three groups by using one qualitative and two quantitative methods. The two-tailed student *t* test was used to compare continuous variables and Fisher's exact test for discrete variables. The DSRs among groups were evaluated with Tukey-Kramer test (alpha value of 0.05 was adopted). A p value <0.05 was considered statistically significant.

Results

Patient characteristics are listed in Table 1. There were no differences in sex and gender among the three groups.

The results obtained with the qualitative method (Table 1) showed that 4 (40%) LDS and 16 (80%) MFS patients possessed DE, but none of the control subject did. DE were thus more frequently observed in LDS and MFS than in control ($p = 0.0077$ and <0.001, respectively). There was no anterior meningocele in LDS or control, but one in MFS, while one lateral meningocele was observed in LDS (Fig. 2) and five in MFS, but none in control.

According to findings obtained with method-1 (Table 1), 5 (50%) LDS and 15 (75%) MFS patients possessed DE, and none of the control subjects did. Higher prevalence of DE in LDS and MFS than in control was also observed with this diagnostic method ($p = 0.0018$ and <0.0001, respectively).

According to findings obtained with method-2 (Table 1), LDS (at L2) and MFS (at L5, S1) patients had a higher prevalence of DE than control. Seven (70%) LDS and 17 (85%) MFS showed the presence of DE and one (5%) control also showed DE. Most MFS patients diagnosed with method-2 had DE at S1or L5 while few showed DE at other levels. In addition, LDS patients showed a diffusely wide dura from L1 through to S1 except for L4. The values for DSR are also listed in Table 2.

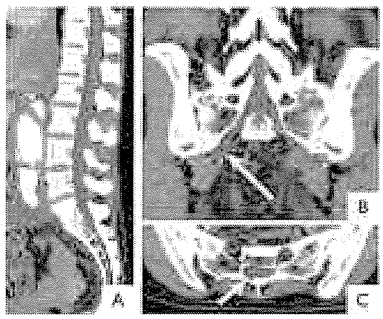

Figure 2. CT images of 46-year-old female with Loeys-Dietz syndrome. Sagittal image of the normal dura (A). Coronal image of right lateral meningocele (arrow) (B). Axial image at S1 shows asymmetric dilatation of the dura (arrow) (C). In this case, visual inspection could detect dural ectasia, but quantitative evaluation could not.
doi:10.1371/journal.pone.0075264.g002

Discussion

DE usually occurs in connective tissue diseases, and was one of the major diagnostic criteria for MFS [6]. DE is no longer a critical criterion for MFS; however, DE still is important because it is used in the scoring system in the revised version [7]. While the importance of DE is well recognized in MFS, its prevalence in LDS is unknown. Although there is at present no standardized diagnostic method for DE in LDS, some qualitative [6,8] and quantitative methods [9,12,13] have been used. In contrast to findings for MFS, only a few reports have dealt with the prevalence of DE in LDS [1,10,11]. Our study showed that LDS had a wider dural sac than control and the prevalence of DE in LDS was significantly higher than in control regardless of which

Table 1. Patient characteristics and prevalence of DE determined with qualitative and quantitative methods.

	LDS (n = 10)	MFS (n = 20)	Control (n = 20)	Difference*
Gene abnormality	TGFBR-1 or -2	FBN-1		
Gender (m:f)	6:4	12:8	12:8	NS
Age (y)	36.3±12.6	37.1±11.2	36.1±8.6	NS
No. of DE identified with qualitative method				
DE-positive	4 (40)	16 (80)	0 (0)	a, (p = 0.04); b, (p = 0.0077); c, (p<0.0001)
No. of DE identified with method-1				
DE-positive	5 (50)	15 (75)	0 (0)	b, (p = 0.0018); c, (p<0.0001)
No. of DE identified with method-2				
DE-positive at any level	7 (70)	17 (85)	1 (5)	b, (p = 0.00068); c, (p<0.0001)
L1	4 (40)	3 (15)	1 (5)	
L2	3 (30)	3 (15)	0 (0)	
L3	3 (30)	3 (15)	0 (0)	
L4	0 (0)	4 (20)	0 (0)	
L5	2 (20)	7 (35)	1 (5)	
S1	6 (60)	16 (80)	0 (0)	

LDS, Loeys-Dietz syndrome; MFS, Marfan syndrome; DSR, dural sac ratio; DE, dural ectasia; NS, not significant; a, difference between LDS and MFS; b, difference between LDS and control; c, difference between MFS and control.
Difference*, In this column, p values are shown. Differences were not tested for each level from L1 to S1.
doi:10.1371/journal.pone.0075264.t001

Table 2. Mean DSR values.

	LDS (n = 10)	MFS (n = 20)	Control (n = 20)	CI*
L1	0.56±0.08	0.52±0.12	0.48±0.06	NS
L2	0.53±0.09	0.49±0.12	0.45±0.06	b, 0.0004−0.17
L3	0.48±0.08	0.45±0.09	0.42±0.06	NS
L4	0.45±0.07	0.47±0.11	0.44±0.02	NS
L5	0.53±0.10	0.56±0.15	0.43±0.08	c, 0.04−0.22
S1	0.60±0.11	0.88±0.54	0.40±0.07	c, 0.21−0.74

DSR, dural sac ratio; LDS, Loeys-Dietz syndrome; MFS, Marfan syndrome; DE, dural ectasia; NS, not significant; a, difference between LDS and MFS; b, difference between LDS and control; c, difference between MFS and control. CI*, this column shows the confidence interval for significant differences.
doi:10.1371/journal.pone.0075264.t002

diagnostic method was used. According to the findings obtained with the methods used in our study, the prevalence of DE in LDS varied from 40 to 70%. This prevalence is higher than the 16% reported by Rodrigues et al. [10]. Although their report does not mention any details of diagnostic criteria for DE, they also used CT images. The reason for the difference between the two studies is not clear. In this study, DE was positive in 75–85% for MFS and 0–5% for NML. In a clinical setting, the differential diagnosis of LDS from MFS is problematic. Although the difference in DE frequency observed using a qualitative method is significant ($p = 0.04$) between LDS and MFS, the differences between method-1 and method-2 are not significant. This result shows that only knowing DE frequency would not be helpful when attempting to distinguish LDS from MFS. Further examination is needed to determine the differences that exist between these two genetic vascular disorders in addition to DE frequency.

Some reports about DE in MFS have emphasized quantitative methods because cutoff values can be used more uniformly than with qualitative methods [12,18]. However Lundby et al. reported that qualitative signs were very useful because 11.5% of their patients would not have been diagnosed with DE if lateral menigocele had not been adopted as a sign of DE [17]. Anterior and lateral meningocele has been identified as a strong qualitative indicator of DE in many studies [6,9,17]. We also propose the use of visual evaluation of DE, as presented in Fig. 2, because two (20%) LDS and three (6%) MFS patients were diagnosed by means of qualitative assessment although they were not diagnosed as such with method-1. As well as anterior or lateral meningocele, asymmetric dilatation such as scalloping of the vertebral body or widening of the neural foramina cannot be detected with qualitative evaluation in the mid-sagittal plain. In this study, the prevalence of anterior and lateral meningocele was lower than previously reported. This may be due to the lower contrast resolution of CT compared with MRI, which may lead to misdiagnosis of some meningoceles.

A higher prevalence of DSD at S1 than that at L4 (method-1) was used as a quantitative diagnostic method for DE [9] and resulted in assessment with high inter-observer agreement ($\kappa = 0.77$) [17]. This parameter can be easily and reliably measured in a routine clinical setting on CT and MRI, and previous studies have reported that it is also a useful marker for DE in [9,18]. Our result showed that five (50%) LDS and 15 (75%) MFS patients showed DE with this quantitative method in contrast to control (0%), which is consistent with previously reported findings. While this parameter is thus a useful diagnostic tool, it can be somewhat problematic in that the difference in DSD at L4 and S1 is often very small. There were a total of seven cases among the LDS and MFS patients in our study with differences of less than 2 mm. It is also problematic that diffuse ectasis throughout the lumbosacral regions is not detected with this method.

DSR (method-2), which Oosterhof et al. firstly described in 2001 [12], has been used to assess DE in recent studies [13,17]. The authors concluded that a combination of DSR above a given cutoff value at level L3 and S1 could be used to identify MFS with 95% sensitivity and 98% specificity. However, their method has been tested in later studies, but similar results have not been obtained [18,19]. Habermann et al. found a sensitivity of 56% and a specificity of 65% with an optimal cutoff value of 0.51 at S1 [18]. They suggested that some of the differences in cutoff values and accuracy were secondary to the age differences of the subjects enrolled in the two studies. Cutoff values depend on the characteristics of the control group such as age, ethnos, and diagnostic modality (i.e. CT or MRI). The main purpose of the cutoff values adopted for our study (means+2 SD of controls) was therefore to reduce the influence of such dependence. The DSRs reported by Lundby were 0.45, 0.43, 0.42, and 0.41 at L3, 4, 5, and S1, respectively [17], and those reported by Oosterhof were 0.48, 0.40, 0.35, 0.34, 0.32, and 0.35 at L1, 2, 3, 4, 5 and S1, respectively, [12]. These results were thus not so different from ours. By using our cutoff values, we identified DE in seven (70%) LDS and 17 (85%) MFS patients. Because most of LDS and MFS patients showed DE at S1, the prevalence of DE obtained with method-2 was equivalent to that obtained with method-1 in our study. As mentioned before, method-1 cannot identify an abnormality when the dilatation is diffuse (i.e., L4 was dilatated as well as S1). As seen in Table 2, LDS patients, in contrast to MFS patients, feature a diffuse dilatation, so that the use of cutoff values may help diagnose the dilatation of DE correctly even in LDS patients. In addition, the finding of the diffuse distribution of DE may help to identify LDS and distinguish it from MFS, although the difference between LDS and MFS was not significant in our study.

In a recent report, Soylen et al. reported 100% sensitivity and 94.7% specificity for a novel quantitative method using MRI images [13]. They adopted the value calculated by multiplying longitudinal diameter by wide diameter of the dura in axial plane for each level. They compared their results with those of Ahn and Oosterhof and found that sensitivity was equivalent for the three methods but their specificity was superior to Oosterhof's. We also adopted their qualitative method using CT images (unpublished data). While our results showed that many LDS and MFS patients had DE, the prevalence was very similar to that assessed with method-2. Soylen et al.'s method has a good diagnostic performance, but the measurements are rather time-consuming, so that the method proposed by Ahn or Oosterhof may be satisfactory for clinical settings.

Compared with CT, MRI is superior in quality of contrast resolution, especially in visualization of soft tissue. Therefore, most previous studies have used MRI imaging for the evaluation of DE [9,12,13]. However, thin slice data can now be obtained easily with CT, and MPR images derived form CT make it possible to analyze objects easily from any plane. In our institution, we usually reconstruct CT images of 2 mm slice thickness and diagnose them using a PACS viewer. Under these circumstances, we can reconstruct MPR images and analyze them within 5 min per patient. We applied MRI criteria for DE to our CT measurements. This is because we believed that these MRI criteria could be used with current CT images. As explained above, lateral and anterior meningocele constitutes an important finding of DE [17].

Reconstructed MPR CT images can also be used for the evaluation of both lateral and anterior meningocele. The fact that T2-weighted images on MRI are superior for detecting abnormalities with a water component makes the detection of lateral and anterior meningocele using MRI feasible. Moreover, careful reading of axial and MPR images of CT is sure to improve the detectability of anterior and lateral meningocele.

In this study, LDS showed a higher prevalence of DE than controls. If the presence of DE turns out to be a useful finding for differentiating LDS from controls, it may well become one of the diagnostic criteria. However, further study is needed to evaluate its diagnostic performance and feasibility.

Our study has certain limitations. First, while the number of patients in our study was very small, it is comparable with the numbers used in other studies. LDS patients in this study were consecutively recruited and represented the maximum number of this type of patient at that time. However, our study did not include patients aged <20 because there were no patients of that age in our hospital. This may have caused a patient selection bias, thereby influencing our results. Our results for MFS and controls were comparable with those of a study comprising a large number of MFS patients [17]. For LDS, on the other hand, further studies with a large number of subjects is necessary. Second, because to some extent DE develops with age, some patients may be without DE in spite of gene abnormalities. In this respect, we did not calculate either the sensitivity or specificity for the evaluation of the diagnostic performance against the genetic diagnosis as a reference standard. Of course, the prevalence of DE may fluctuate to some extent depending on the characteristics of the groups.

Conclusions

LDS as well as MFS showed a higher prevalence of DE than controls. The prevalence of DE in LDS varied from 40 to 70% depending on different qualitative and quantitative methods. These findings indicate that DE has the potential to become a diagnostic criterion for LDS.

Author Contributions

Conceived and designed the experiments: AKK HN KS. Performed the experiments: MH. Analyzed the data: AKK. Contributed reagents/materials/analysis tools: HM TM. Wrote the paper: AKK.

References

1. Loeys BL, Chen J, Neptune ER, Judge DP, Podowski M, et al. (2005) A syndrome of altered cardiovascular, craniofacial, neurocognitive and skeletal development caused by mutations in TGFBR1 or TGFBR2. Nat Genet 37: 275–281.
2. Loeys BL, Schwarze U, Holm T, Callewaert BL, Thomas GH, et al. (2006) Aneurysm syndromes caused by mutations in the TGF-beta receptor. N Engl J Med 355: 788–798.
3. Kono AK, Higashi M, Morisaki H, Morisaki T, Tsutsumi Y, et al. (2010) High prevalence of vertebral artery tortuosity of Loeys-Dietz syndrome in comparison with Marfan syndrome. Jpn J Radiol 28: 273–277.
4. Singh KK, Rommel K, Mishra A, Karck M, Haverich A, et al. (2006) TGFBR1 and TGFBR2 mutations in patients with features of Marfan syndrome and Loeys-Dietz syndrome. Hum Mutat 27: 770–777.
5. Dietz HC, Pyeritz RE, Hall BD, Cadle RG, Hamosh A, et al. (1991) The Marfan syndrome locus: confirmation of assignment to chromosome 15 and identification of tightly linked markers at 15q15-q21.3. Genomics 9: 355–361.
6. De Paepe A, Devereux RB, Dietz HC, Hennekam RC, Pyeritz RE (1996) Revised diagnostic criteria for the Marfan syndrome. Am J Med Genet 62: 417–426.
7. Loeys BL, Dietz HC, Braverman AC, Callewaert BL, De Backer J, et al. (2010) The revised Ghent nosology for the Marfan syndrome. J Med Genet 47: 476–485.
8. Fattori R, Nienaber CA, Descovich B, Ambrosetto P, Reggiani LB, et al. (1999) Importance of dural ectasia in phenotypic assessment of Marfan's syndrome. Lancet 354: 910–913.
9. Ahn NU, Sponseller PD, Ahn UM, Nallamshetty L, Rose PS, et al. (2000) Dural ectasia in the Marfan syndrome: MR and CT findings and criteria. Genet Med 2: 173–179.
10. Rodrigues VJ, Elsayed S, Loeys BL, Dietz HC, Yousem DM (2009) Neuroradiologic manifestations of Loeys-Dietz syndrome type 1. AJNR Am J Neuroradiol 30: 1614–1619.
11. Akutsu K, Morisaki H, Takeshita S, Sakamoto S, Tamori Y, et al. (2007) Phenotypic heterogeneity of Marfan-like connective tissue disorders associated with mutations in the transforming growth factor-beta receptor genes. Circ J 71: 1305–1309.
12. Oosterhof T, Groenink M, Hulsmans FJ, Mulder BJ, van der Wall EE, et al. (2001) Quantitative assessment of dural ectasia as a marker for Marfan syndrome. Radiology 220: 514–518.
13. Soylen B, Hinz K, Prokein J, Becker H, Schmidtke J, et al. (2009) Performance of a new quantitative method for assessing dural ectasia in patients with FBN1 mutations and clinical features of Marfan syndrome. Neuroradiology 51: 397–400.
14. De Paepe A (1999) Dural ectasia and the diagnosis of Marfan's syndrome. Lancet 354: 878–879.
15. Pyeritz RE, Fishman EK, Bernhardt BA, Siegelman SS (1988) Dural ectasia is a common feature of the Marfan syndrome. Am J Hum Genet 43: 726–732.
16. Oren M, Lorber B, Lee SH, Truex RC Jr, Gennaro AR (1977) Anterior sacral meningocele: report of five cases and review of the literature. Dis Colon Rectum 20: 492–505.
17. Lundby R, Rand-Hendriksen S, Hald JK, Lilleas FG, Pripp AH, et al. (2009) Dural ectasia in Marfan syndrome: a case control study. AJNR Am J Neuroradiol 30: 1534–1540.
18. Habermann CR, Weiss F, Schoder V, Cramer MC, Kemper J, et al. (2005) MR evaluation of dural ectasia in Marfan syndrome: reassessment of the established criteria in children, adolescents, and young adults. Radiology 234: 535–541.
19. Rose PS, Levy HP, Ahn NU, Sponseller PD, Magyari T, et al. (2000) A comparison of the Berlin and Ghent nosologies and the influence of dural ectasia in the diagnosis of Marfan syndrome. Genet Med 2: 278–282.

Surgical Experience With Aggressive Aortic Pathologic Process in Loeys-Dietz Syndrome

Yutaka Iba, MD, Kenji Minatoya, MD, Hitoshi Matsuda, MD, Hiroaki Sasaki, MD, Hiroshi Tanaka, MD, Hiroko Morisaki, MD, Takayuki Morisaki, MD, Junjiro Kobayashi, MD, and Hitoshi Ogino, MD

Departments of Cardiovascular Surgery and Bioscience and Genetics, National Cerebral and Cardiovascular Center, Osaka; Department of Cardiovascular Surgery, Tokyo Medical University, Tokyo, Japan

Background. Loeys-Dietz syndrome (LDS) is a recently recognized connective tissue disorder (CTD) caused by mutations in *transforming growth factor-beta receptor (TGFBR)1* and *TGFBR2*. Surgical outcomes of aortic repair in patients with LDS are poorly known.

Methods. We enrolled 16 patients with *TGFBR* mutations identified by gene analysis in this study. Between 1993 and 2011, they underwent 41 aortic surgical procedures. Ten patients (group D: dissection group) underwent aortic repair for acute or chronic aortic dissection as a first surgical intervention, and 6 patients (group N: nondissection group) underwent surgical treatment for aortic root dilatation. The mean follow-up period was 103.7 ± 92.3 months (range, 2– 276 months).

Results. There were no in-hospital deaths. In group N, valve-sparing root replacement (VSRR) was performed in all patients. The residual aorta in 9 patients (90%) from group D required further repairs, 3 times on average. Moreover, in 4 patients (40%), the aorta was entirely replaced in serial procedures. In group N, aortic dissection occurred in only 1 patient (17%). The aortic event-free rates at 5 years were 40% in group D and 80% in group N, respectively ($p = 0.819$). One late death due to arrhythmia occurred 1 month after VSRR. The cumulative survival rates at 5 years were 100% in group D and 83% in group N, respectively ($p = 0.197$).

Conclusions. Surgical outcomes for patients with LDS were satisfactory. Once aortic dissection occurred, the aorta expanded rapidly, requiring further operations. Therefore, early surgical intervention may improve prognosis by preventing a fatal aortic event.

(Ann Thorac Surg 2012;94:1413–7)

Loeys-Dietz syndrome (LDS) is a recently recognized connective tissue disorder (CTD) first described by Loeys and colleagues in 2005 [1] and resulting from mutations in *transforming growth factor-beta receptor (TGFBR)1* and *TGFBR2*. Phenotypic characteristics include arterial tortuosity, aortic aneurysms and dissections, ocular hypertelorism, bifid uvula, and cleft palate [1–3]. Of these characteristics, aortic lesions are considered to have the greatest influence on prognosis, similar to other CTDs such as Marfan's syndrome (MFS) or vascular-type Ehlers-Danlos syndrome. Indeed, some reports indicate that the aortic pathologic process in LDS is more aggressive and widespread than it is in MFS [2]. However surgical results and the postoperative prognosis of aortic repair in patients with LDS are not well known, although most patients require aortic operations.

In this study, we describe our surgical experience with aortic repair in patients with LDS with a severe aortic pathologic process.

Patients and Methods

We performed genetic analysis in patients undergoing aortic surgical procedures at our center who were suspected of having a CTD because of young age, family history, typical annuloaortic ectasia (AAE), and so on. On the basis of the results, we enrolled 16 patients with mutations in *TGFBR1* or *TGFBR2* in this study (Table 1). Between 1990 and 2011, these patients collectively underwent 41 aortic operations. Mean age at the first operation was 31.4 ± 11.3 years. Nine patients had mutations in *TGFBR1* and 7 had mutations in *TGFBR2*. Ten patients underwent their first aortic operations after aortic dissection (group D: dissection group). In group D, indication for first surgical intervention was chronic type B aortic dissection in 6 patients and acute type A aortic dissection in 4 patients. Patients included a 20-year-old woman who at 19 weeks of pregnancy required urgent operation for acute type A aortic dissection. The first surgical intervention in the remaining 6 patients was for AAE without aortic dissection (group N: nondissection group).

Data were collected from hospital admission and outpatient medical records and telephone interviews. All patients were regularly assessed, either at our center or by a local cardiologist. The follow-up rate was 100%, and

Accepted for publication May 25, 2012.

Presented at the Poster Session of the Forty-eighth Annual Meeting of The Society of Thoracic Surgeons, Fort Lauderdale, FL, Jan 28–Feb 1, 2012.

Address correspondence to Dr Iba, 5-7-1 Fujishirodai, Suita, Osaka, 565-8565, Japan; e-mail: iba@hsp.ncvc.go.jp.

Published by Elsevier Inc

0003-4975/$36.00
http://dx.doi.org/10.1016/j.athoracsur.2012.05.111

Abbreviations and Acronyms

AAE = annuloaortic ectasia
CSF = cerebrospinal fluid
CTD = connective tissue disorder
LDS = Loeys-Dietz syndrome
MFS = Marfan's syndrome
TGFBR = transforming growth factor-beta receptor
VSRR = valve-sparing root replacement

the mean follow-up period was 103.7 ± 92.3 months (range, 2–276 months). Our institution approved this retrospective study, and patient consent for our study was obtained either at the time of operation or when the patients came as outpatients.

Continuous variables were expressed as mean ± standard deviation and compared using the Student's *t* test. Categorical data were compared using Fisher's exact test. Survival and aortic event-free rates were estimated using the Kaplan-Meier method, and differences between each group were determined by log-rank analysis. *p* values of less than 0.05 were considered significant. Statistical analysis was performed using SPSS, version 17.0 for Windows (IBM SPSS Inc, Chicago, IL).

Results

No operative or in-hospital deaths occurred in our series. During postoperative hospitalization, there were 3 cerebrovascular events. Subdural hematoma occurred in 2 patients; 1 underwent descending thoracic aorta replacement and the other underwent thoracoabdominal aortic replacement for chronic type B aortic dissection. A third patient, who underwent emergency arch repair for acute type A aortic dissection, was diagnosed with cerebral infarction with right hemiparesis. The woman who needed emergency operation for acute aortic dissection during pregnancy safely gave birth to a baby 5 months after operation. In group N, valve-sparing root replacement (VSRR) was carried out in all 6 patients, and no major complications occurred in this group during hospitalization.

Follow-up results after the aortic procedures are shown in Table 2. Nine patients (90%) in group D required further aortic operations. Patients underwent a mean of 3 aortic procedures. Moreover, the aorta in 4 patients was entirely replaced through serial aortic operations. In group N, only 2 patients (33%) underwent further aortic repair. One patient underwent elective abdominal aortic replacement for an aneurysm of the abdominal aorta and bilateral common iliac artery, whereas another patient was diagnosed with acute dissection from the aortic arch to the terminal aorta 6 years after VSRR. After this, she needed a further aortic operation for dilatation of the dissected aorta. She finally achieved total aortic replacement 1 year after aortic dissection. The overall aortic event-free rates at 5 and 10 years were 46.4% and 18.6%, respectively (Fig 1). In the follow-up, there was only 1 late death resulting from arrhythmia. This patient, who was discharged uneventfully 12 days after VSRR for AAE, died suddenly 32 days after operation. The cumulative survival rate at 5 years was 93.8% in all patients (Fig 2).

Comment

Some phenotypic characteristics of LDS, such as aortic tortuosity and skeletal abnormality, overlap with those of MFS, a representative CTD, suggesting that to date LDS has been regarded as an MFS-like disease or practically treated as MFS. However important phenotypic differences have been described [1–4]. Characteristic craniofacial findings of LDS, such as hypertelorism, cleft palate, or bifid uvula, are seldom found in patients with MFS. In addition, some patients with LDS are not so tall, and lens dislocation, which is typical in MFS, is uncommon in patients with LDS.

Table 1. Patient Characteristics

Characteristic	Group D n = 10	Group N n = 6	*p* Value
Male sex	3	4	0.152
Mean age at first operation	36.0 ± 12.2	23.7 ± 5.4	0.357
Genetic mutation			
TGFBR 1	6	3	0.696
TGFBR 2	4	3	
Mean number of aortic operations	3.0 ± 1.2	1.8 ± 1.5	0.125
Type of aortic operation			
Root replacement			
VSRR	3[a]	6	
Bentall	7[a]	0	
Arch repair	7	1	
DTAA repair	5	1	
TAAA repair	5	1	
AAA repair (infrarenal)	3	2	
Preoperative AI before VSRR			
None	0	1	
Trivial	1	2	
Mild	2	2	
Moderate	0	1	
Severe	0	0	
Postoperative AI after VSRR			
None	1	4	
Trivial	2	2	
Mild	0	0	
Moderate	0	0	
Severe	0	0	

[a] Including concomitant arch repair.

AAA = abdominal aortic aneurysm; AI = aortic insufficiency; DTAA = descending thoracic aortic aneurysm; TAAA = thoracoabdominal aortic aneurysm; *TGFBR = transforming growth factor beta receptor;* VSRR = valve-sparing root replacement.

Table 2. Surgical History of Each Patient

Group	Patients	Indication of First Operation	Maximum Diameter of Aorta (mm)	First Operation	Second Operation		Third Operation		Fourth Operation		Fifth Operation		Total Aortic Replacement
D	1	Chronic AD (B)	60	DTAA repair	VSRR (remodeling) + TAR	(49)	TAAA repair	(53)	Bentall	(159)	...		Yes
	2	Chronic AD (B)	60	AAA repair	HAR	(5)	DTAA repair	(46)	TAAA repair	(85)	Bentall + TAR	(154)	Yes
	3	Chronic AD (B)	N/A	DTAA repair	TAR	(41)	TAAA repair	(62)	Bentall + MVR	(104)	...		Yes
	4	Chronic AD (B)	45	AAA repair	...		...		...		...		No
	5	Chronic AD (B)	60	TAR	AAA repair	(110)	TAAA repair	(116)	...		...		No
	6	Chronic AD (B)	59	DTAA repair	Bentall + TAR	(13)	TAAA repair	(26)	...		...		Yes
	7	Acute AD (A)	N/A	Bentall	TAR	(132)	RedoBentall	(195)	Redo Bentall	(196)	...		No
	8	Acute AD (A)	78	HAR	VSRR	(51)	...		...		...		No
	9	Acute AD (A)	N/A	HAR	VSRR + TAR	(67)	...		...		...		No
	10	Acute AD (A)	...	TAR	DTAA repair	(1)	...		...		...		No
N	11	AAE	57	VSRR	TAR	(79)	DTAA repair		AAA repair		TAAA repair		Yes
	12	AAE	50	VSRR	...		...		...		...		No
	13	AAE	45	VSRR	...		...		...		...		No
	14	AAE	48	VSRR	...		...		...		...		No
	15	AAE	58	VSRR	...		...		...		...		No
	16	AAE	60	VSRR	AAA repair	(3)	...		...		...		No

Numbers in parentheses indicate months from first operation.

AAA = abdominal aortic aneurysm; AAE = annuloaortic ectasia; AD (A) = aortic dissection, type A; AD (B) = aortic dissection, type B; DTAA = descending thoracic aortic aneurysm; HAR = hemiarch replacement; MVR = mitral valve replacement; N/A = not available; TAAA = thoracoabdominal aortic aneurysm; TAR = total arch replacement; VSRR = valve-sparing root replacement.

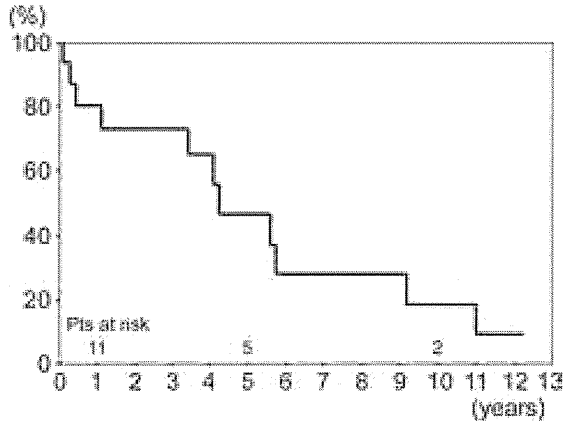

Fig 1. Freedom from aortic reintervention for all patients (Pts) after first aortic operation.

TGFBR molecules are associated with cardiovascular development and function: *TGFBR1* or *TGFBR2* mutations influence collagen deposition and elastin organization in the extracellular matrix. With respect to the histopathologic features of aortic specimens, fragmentation of elastic fibers is frequently seen in patients with both LDS and MFS. Maleszewski and colleagues [5], who examined aortic specimens of patients with both LDS and MFS in detail, showed that high collagen deposition and medial degeneration of the diffuse type with relatively little medial degeneration of the cystic type helps differentiate LDS from MFS. Indeed, in most of our patients, the pathologic findings showed diffuse medial degeneration in addition to fragmentation of elastic fibers. These changes in the media make the aortic wall fragile and lead to arterial tortuosity with aortic aneurysms and dissections.

In patients with LDS, management of aortic lesions is vital for prognosis, as it is in other CTDs. Most patients in group D, who underwent initial aortic repair after aortic dissection, needed further aortic operations because the dissected aorta of patients with LDS dilates easily. As a result, 40% of patients had their aortas replaced entirely in several rounds of aortic repair. Conversely, all patients in group N, in whom aortic lesions were detected before aortic events occurred, underwent aortic operations for AAE. For all patients in group N, VSRR with a reimplantation technique using a polyester tube graft with prefashioned pseudosinuses (Gelweave Valsalva graft; Vascutek, Renfrewshire, Scotland, UK) could be carried out successfully, and postoperative echocardiography revealed less than trivial aortic regurgitation. Patel and colleagues [6] demonstrated that midterm results of VSRR for patients with LDS are encouraging, and we also believe that it is an effective surgical option, especially for young patients.

In our series, there were 2 cases of subdural hematoma postoperatively. One occurred after descending thoracic aorta replacement. In our strategy, at the time of replacement of the descending or thoracoabdominal aorta, a cerebrospinal fluid (CSF) drainage catheter is inserted, and motor-evoked potentials are monitored for spinal cord protection. When the amplitudes of the motor-evoked potentials decrease or recover insufficiently, CSF drainage commences. Therefore the cause of the subdural hematoma might be considered to be related to rapid drainage of CSF performed for spinal cord protection. The other patient, who underwent thoracoabdominal aortic replacement for chronic type B aortic dissection, experienced subdural hematoma 2 days postoperatively, although no intracranial lesions were observed on preoperative brain computed tomography. Intracranial aneurysms have been reported as 1 of the arterial lesions related to LDS [7, 8]. In our patient, magnetic resonance or computed tomography angiography for intracranial lesions had not been performed preoperatively; however, we should pay attention to the existence of such intracranial aneurysms.

In 1 particularly interesting case (patient 11, Table 2), aortic dissection occurred from the aortic arch to the abdominal aorta about 6 years after VSRR. The patient had received regular follow-ups and a computed tomographic scan after the initial operation; the maximum diameter of the aortic arch was only 39 mm on a computed tomographic scan taken 1 month before dissection (Fig 3). After this, she underwent total aortic replacement through serial aortic repairs over 1 year. This experience may suggest that a more aggressive strategy be considered to concomitantly repair the aortic arch at the root operation for prevention of future type A aortic dissection, as Augoustides and colleagues [9] advocated. Further follow-up is therefore necessary.

Clinical strategies for aggressive aortic lesions in LDS have yet to be established because there are still few large-scale reports about surgical results and prognoses. However Williams and colleagues [10], who have much experience in aortic operations for patients with LDS, suggested that the threshold for surgical intervention in adult patients with LDS is 4 cm for the aortic root and abdominal aorta and 5 cm for the descending thoracic aorta or for rapid expansion (> 0.5 cm/year) regardless of location. This surgical approach is considered more ag-

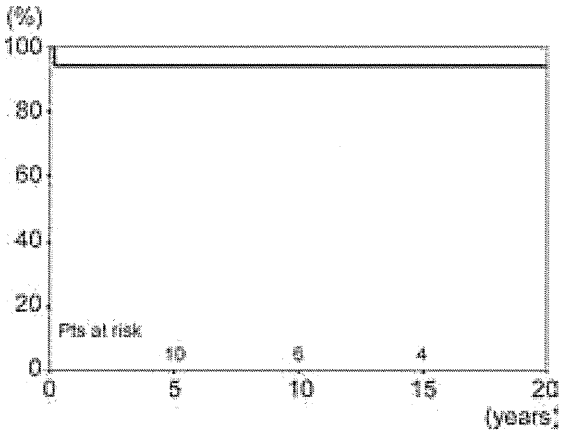

Fig 2. Kaplan-Meier survival curve for all patients (Pts) after first aortic operation.

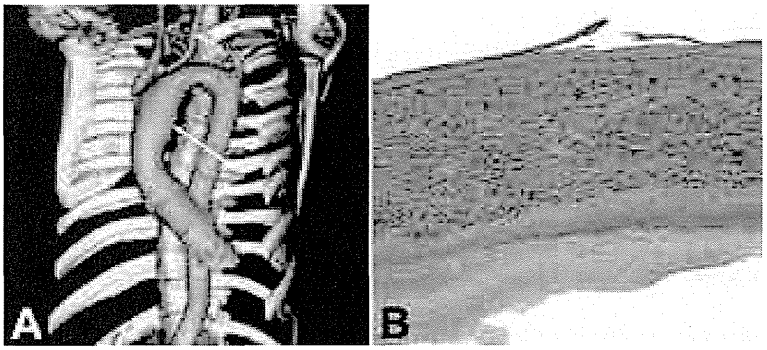

Fig 3. (A) Computed tomographic scan, obtained 1 month before aortic dissection, revealed the maximum diameter of the aortic arch to be 39 mm, with fusiform mild dilatation (arrow). (B) The histopathologic findings of the aortic wall showed diffuse medial degeneration and elastin fragmentation of media (elastica van Gieson stain ×100).

gressive than that for patients with MFS. In our experience, operative results for patients with LDS were satisfactory; moreover, once aortic dissection occurs, most patients need repeated aortic operations [11]. Before this disease was recognized, we had considered surgical indications and management of LDS in the same way as those for MFS. However for the past few years, in which we have recognized the fragile nature of aortic lesions in patients with LDS, we have been adopting a more aggressive strategy for surgical intervention. Therefore we believe that early surgical intervention may improve prognosis by preventing fatal aortic events.

Endovascular treatment should be considered a contraindication in patients with LDS because use of the native aorta as a landing zone carries the risk of potential dilatation. However a recent noteworthy case report describes hybrid therapy, combining open aortic repair and endovascular stent grafting [12].

This study has some limitations. First, our experience with this recently recognized arteriopathy is still limited. Second, this study is retrospective in nature.

In conclusion, we should recognize the aggressive aortic pathologic process in this syndrome, and a clinical management strategy should be established by accumulating further clinical experience.

References

1. Loeys BL, Chen J, Neptune ER, et al. A syndrome of altered cardiovascular craniofacial neurocognitive and skeletal development caused by mutations in TGFBR1 and TGFBR2. Nat Genet 2005;37:275–81.
2. Loeys BL, Schwartze U, Holm T, et al. Aneurysm syndrome caused by mutations in the TGF-beta receptor. N Engl J Med 2006;355:788–98.
3. Van Hemelrijk C, Renard M, Loeys B. The Loeys-Dietz syndrome: an update for the clinician. Curr Opin Cardiol 2010; 25:546–51.
4. Aalberts JJ, van der Berg MP, Bergman JE, et al. The many faces of aggressive aortic pathology: Loeys-Dietz syndrome. Neth Heart J 2008;16:299–304.
5. Maleszewski JJ, Miller DV, Lu J, Dietz HC, Halushka MK. Histopathologic findings in ascending aortas from individuals with Loeys-Dietz syndrome. Am J Surg Pathol 2009;33: 194–201.
6. Patel ND, Arnaoutakis GJ, George TJ, et al. Valve-sparing aortic root replacement in Loeys-Dietz syndrome. Ann Thorac Surg 2011;92:556–61.
7. Levitt MR, Morton RP, Mai JC, Ghodke B, Hallam DK. Endovascular treatment of intracranial aneurysms in Loeys-Dietz syndrome. J Neurointerv Surg 2011 Dec 22. [Epub ahead of print].
8. Rahme RJ, Adel JG, Bendok BR, Bebawy JF, Gupta DK, Batjer HH. Association of intracranial aneurysm and Loeys-Dietz syndrome: case illustration, management, and literature review. Neurosurgery 2011;69:e488–92.
9. Augoustides JG, Plappert T, Bavaria JE. Aortic decision-making in the Loeys-Dietz syndrome: aortic root aneurysm and a normal-caliber ascending aorta and aortic arch. J Thorac Cardiovasc Surg 2009;138:502–3.
10. Williams JA, Loeys BL, Nwakanma LU, et al. Early surgical experience with Loeys-Dietz: a new syndrome of aggressive thoracic aortic aneurysm disease. Ann Thorac Surg 2007;83: S757–63.
11. Williams ML, Wechsler SB, Hughes GC. Two-stage total aortic replacement for Loeys-Dietz syndrome. J Card Surg 2010;25:223–4.
12. Williams JB, McCann RL, Hughes GC. Total aortic replacement in Loeys-Dietz syndrome. J Card Surg 2011;26:304–8.

Cardiology in the Young (2012), 22, 116–119
doi:10.1017/S1047951111001028

Brief Report

Prenatal complex congenital heart disease with Loeys–Dietz syndrome

Yukiko Kawazu,[1] Noboru Inamura,[1] Futoshi Kayatani,[1] Nobuhiko Okamoto,[2] Hiroko Morisaki[3]

[1]Department of Pediatric Cardiology; [2]Department of Medical Genetics, Osaka Medical Center and Research Institute for Maternal and Child Health, Izumi; [3]Department of Bioscience and Genetics, National Cerebral and Cardiovascular Center Research Institute, Suita, Osaka, Japan

Abstract We report an infantile case of Loeys–Dietz syndrome prenatally diagnosed with congenital complex heart disease – double outlet right ventricle and interruption of the aortic arch. The patient also showed prominent dilatation of the main pulmonary artery. Emergency bilateral pulmonary artery banding was performed on the 9th day. However, on the 21st day, the patient died of massive bleeding due to rupture of the right pulmonary artery. Subsequently, a mutation of the TGFBR1 gene was detected. As cardiovascular lesions of Loeys–Dietz syndrome appear early and progress rapidly, the prognosis is generally poor. Patients require periodic examination and early intervention with medical therapy such as Losartan administration and surgical therapy. Early genetic screening is thought to be useful for the prediction of complications as well as vascular disease.

Keywords: Prenatal diagnosis; aneurysm; chromosomal anomaly; connective tissue disorder

Received: 25 January 2011; Accepted: 25 May 2011; First published online: 21 July 2011

LOEYS–DIETZ SYNDROME IS A NEWLY RECOGNISED, rare autosomal dominantly inherited connective tissue disorder caused by heterogeneous mutations in the genes encoding the transforming growth factor beta receptor one or two.[1] This syndrome is characterised by the triad of arterial tortuosity, aneurysm or dissections, hypertelorism, and bifid uvula or cleft palate.[2] Here, we present a patient prenatally diagnosed with complex congenital heart disease and confirmed with Loeys–Dietz syndrome after birth.

Case report

A 31-year-old pregnant woman was referred to our paediatric cardiology unit at the 36th week of gestation because of foetal congenital heart disease and dilatation of the pulmonary artery.

Correspondence to: Y. Kawazu, MD, PhD, 840 Murodo-cho Izumi-city, Osaka 594-1101, Japan. Tel: +81 725 56 1220; Fax: +81 725 56 1858; E-mail: kadoy@mch.pref.osaka.jp

The first foetal echocardiography revealed a huge aneurysm of the main pulmonary artery and complex congenital heart disease – double-outlet right ventricle and interruption of the aortic arch (Fig 1). Detailed multi-planar scanning showed that there was no pulmonary valve stenosis, because of no acceleration in pulmonic flow, and no absent pulmonary valve. Therefore, we suspected a connective tissue disorder, such as Marfan syndrome. The foetus was followed up weekly for foetal decompensation and signs of hydrops until the 39th week of gestation, and an elective caesarean section was then performed. The male infant weighed 2834 grams at birth. After delivery, the infant developed dyspnoea and was intubated for artificial ventilation. Subsequently, a cleft of the soft palate and bifid uvula were noted. To treat the interruption of the aortic arch, we started him on a prostaglandin infusion to maintain patent ductus arteriosus and on nitrogen inhalation to prevent pulmonary blood flow increase. Computed tomography and angiocardiography confirmed the heart

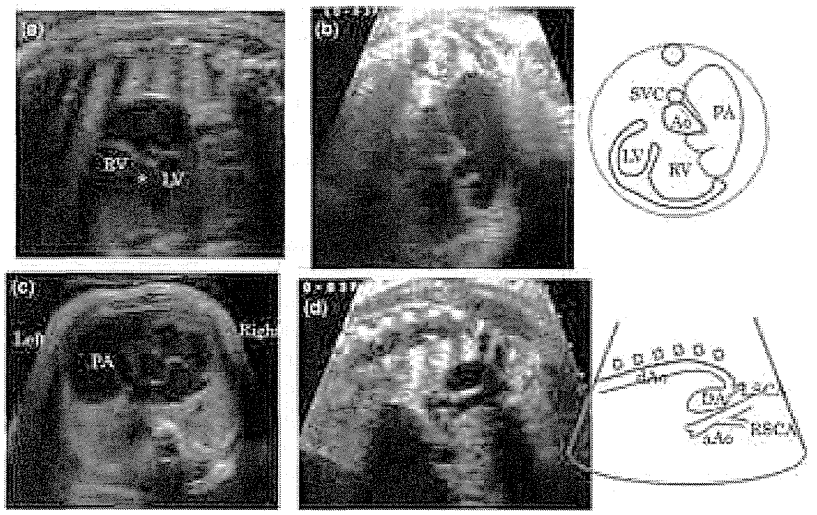

Figure 1.
*Foetal echocardiography shows a large ventricular septal defect (*) of the double-outlet right ventricle (**a**), aneurysmal pulmonary artery (**b**, **c**), and interruption of the aortic arch (**d**). aAo = ascending aorta; Ao = aorta; DA = ductus arteriosus; dAo = descending aorta; LV = left ventricle; LSCA = left subclavian artery; PA = pulmonary artery; RSCA = right subclavian artery; RV = right ventricle; SVC = supra caval vein.*

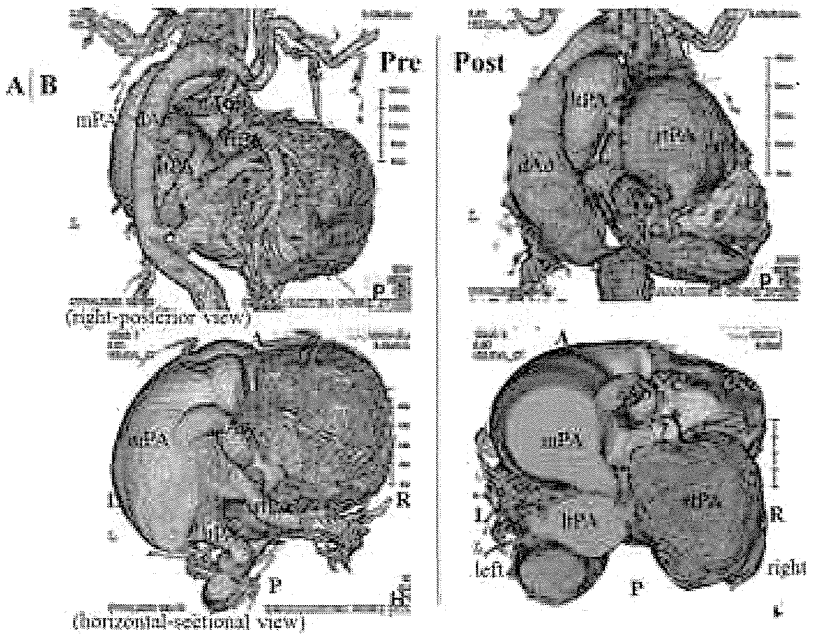

Figure 2.
*Computed tomography (day 0) shows the interruption of the aortic arch and aneurysmal main pulmonary artery before operation (**a**). Computed tomography (day 18) shows progress of the significant expansion of the right and left pulmonary arteries and descending aorta after operation (**b**). A = anterior; aAo = ascending aorta; dAo = descending aorta; L = left; ltpa = left pulmonary artery; P = posterior; mPA = main pulmonary artery; rtPA = right pulmonary artery; R = right.*

disease diagnosed prenatally (Fig 2a). Loeys–Dietz syndrome was strongly suspected because of the presence of cardiovascular lesions, thin skin, and facial appearance. On the 9th day, as the patient had suffered a pulmonary haemorrhage due to pulmonary blood flow increase, emergency bilateral

pulmonary artery banding was performed. However, during surgery, it became apparent that application of normal pulmonary artery banding was impossible because of the very thin condition of the pulmonary artery wall. Therefore, the surgeon performed bilateral banding with the clip, not the usual tape, but the banding was insufficient. This may be a reason why his haemodynamics and respiratory status were not subsequently stable. We again performed computed tomography, which showed a further significant expansion of the right pulmonary artery and descending aorta caused by the pressure of the expanded artery (Fig 2b). Therefore, we started internal use of Losartan. On the 21st day, he developed sudden hypotension and massive bleeding from the thoracic cavity, thought to be caused by right pulmonary rupture, and he died the same day. Subsequently, as the genetic analysis showed p.Thr200Pro (c.598A > C) mutation of the transforming growth factor beta receptor one, he was definitively diagnosed with Loeys–Dietz syndrome. The mutation was *de novo*.

Discussion

Loeys–Dietz syndrome is a recently described connective tissue disorder characterised by aggressive ascending aortic aneurysm and dissection. The clinical features are similar to Marfan syndrome,[3] but this is a more severe syndrome because life-threatening aortic dissection may occur even in early childhood.[4,5] Most patients have the triad of vascular aneurysms, hypertelorism, and bifid or broad uvula/cleft palate associated with variable features. Heterogeneous mutations in the genes encoding for transforming growth factor beta receptors one and two are a consistent finding among affected patients.

In addition, this syndrome shows various cardiovascular manifestations involving not only aortic lesions – such as distortion, aneurysm, and dissections – but also congenital heart diseases.[6] The case described in this report was also complicated with congenital heart disease. The patient's pulmonary artery showed an abnormal expansion because of his heart defect. That is, because he had an interruption of the aortic arch, much more blood than normal flowed through the pulmonary artery and the artery was stressed by "volume overload". Furthermore, the pulmonary artery was stressed by high "pressure overload" because the patient had double-outlet right ventricle and a large ventricular septal defect. It is thought that a pulmonary artery spread for both reasons from the foetal period.

Muramatsu et al[6] reported a case that was complicated with a ventricular septal defect and showed aortic and pulmonary expansion. It is thought that, in the Muramatsu case, the mechanism producing pulmonary artery dilatation was similar to that in the case reported herein. After birth, the patient's pulmonary blood flow increased due to the ventricular septal defect, which led to acute heart failure. He then underwent pulmonary artery banding on the 12th day. After surgery, however, the root of the main pulmonary artery, which was stressed by pressure, had spread in the shape of an aneurysm and intracardiac surgical repair, that is, closure of ventricular septal defect, was performed on the 42nd day. After the operation, the vascular expansion stopped worsening, and in conclusion they recommended early radical operation. However, because our case was a Fontan candidate, he required gradual surgery and radical operation was impossible in early infancy. Therefore, we performed bilateral pulmonary artery banding as a life-saving procedure, but, owing to mural abnormal thinning, the banding was insufficient, and his vascular expansion and thinning progressed, which finally led to explosion and bleeding to death.

In the case reported herein, significant pulmonary expansion from the foetal period led us to suspect a connective tissue disorder such as Marfan syndrome. Viassolo et al[7] reported a similar case in a female patient with Loeys–Dietz syndrome, who showed dilated aortic root from the foetal period. Only aortic dilatation was noted in screening foetal echocardiography at 19 gestational weeks and a connective tissue disease was suspected. She underwent genetic analysis and Loeys–Dietz syndrome was confirmed after birth. At present, the Viassolo case and the one we report herein are the only two cases showing a manifestation of Loeys–Dietz syndrome from the foetal period.

Some cases of Loeys–Dietz syndrome are complicated with congenital heart diseases.[2,6,8] However, those reported hitherto are associated with "simple" congenital heart diseases such as ventricular septal defect, atrial septal defect, patent ductus arteriosus, and aortic bicuspid valve. There is no previous report of Loeys–Dietz syndrome combined with complex congenital heart disease, such as double-outlet right ventricle and interruption of the aortic arch. In such a case, the cardiovascular lesion as an expansion of the great vessels, that is, the aorta or pulmonary artery, may be aggravated during the foetal period. Consequently, the foetus may die in utero. Even if they can be born, their great vessels are continuously or more strongly stressed after birth. Therefore, their arteries expand and finally explode, leading to an early death without undergoing any surgery.

This may be the reason why this is the first reported case of complex heart disease with Loeys–Dietz syndrome.

References

1. Loeys BL, Chen J, Neptune ER, et al. A syndrome of altered cardiovascular, craniofacial, neurocognitive and skeletal development caused by mutations in TGFBR1 or TGFBR2. Nat Genet 2005; 37: 275–281.
2. Loeys BL, Schwarze U, Holm T. Aneurysm syndromes caused by mutations in the TGF-β receptor. N Engl J Med 2006; 355: 788–798.
3. Mizuguchi T, Collod-Beroud G, Akiyama T, et al. Heterozygous TGFBR2 mutations in Marfan syndrome. Nat Genet 2004; 36: 855–860.
4. Yamawaki T, Nagaoka K, Morishige K, et al. Familial thoracic aortic aneurysm and dissection associated with Marfan-related gene mutations: case report of a family with two gene mutations. Intern Med 2009; 48: 555–558.
5. Akutsu K, Morisaki H, Okajima T, et al. Genetic analysis of young adult patients with aortic disease not fulfilling the diagnostic criteria for Marfan syndrome. Circ J 2010; 74: 990–997.
6. Muramatsu Y, Kosho T, Magota M, et al. Progressive aortic root and pulmonary artery aneurysms in a neonate with Loeys–Dietz syndrome type 1B. Am J Med Genet A 2010; 152A: 417–421.
7. Viassolo V, Lituania M, Marasini M, et al. Fetal aortic root dilation: a prenatal feature of the Loeys–Dietz syndrome. Prenat Diagn 2006; 26: 1081–1083.
8. Watanabe Y, Sakai H, Nishimura A, et al. Paternal somatic mosaicism of a TGFBR2 mutation transmitting to an affected son with Loeys–Dietz syndrome. Am J Med Genet A 2008; 146A: 3070–3074.

Acta Oto-Laryngologica, 2013; 133: 345–351

informa
healthcare

ORIGINAL ARTICLE

Genetic analysis of *PAX3* for diagnosis of Waardenburg syndrome type I

TATSUO MATSUNAGA[1], HIDEKI MUTAI[1], KAZUNORI NAMBA[1], NORIKO MORITA[2] & SAWAKO MASUDA[3]

[1]*Department of Otolaryngology, Laboratory of Auditory Disorders, National Institute of Sensory Organs, National Tokyo Medical Center, Tokyo,* [2]*Department of Otolaryngology, Teikyo University School of Medicine, Tokyo and* [3]*Department of Otorhinolaryngology, Institute for Clinical Research, National Mie Hospital, Tsu, Japan*

Abstract

Conclusion: PAX3 genetic analysis increased the diagnostic accuracy for Waardenburg syndrome type I (WS1). Analysis of the three-dimensional (3D) structure of PAX3 helped verify the pathogenicity of a missense mutation, and multiple ligation-dependent probe amplification (MLPA) analysis of *PAX3* increased the sensitivity of genetic diagnosis in patients with WS1. *Objectives:* Clinical diagnosis of WS1 is often difficult in individual patients with isolated, mild, or non-specific symptoms. The objective of the present study was to facilitate the accurate diagnosis of WS1 through genetic analysis of *PAX3* and to expand the spectrum of known *PAX3* mutations. *Methods:* In two Japanese families with WS1, we conducted a clinical evaluation of symptoms and genetic analysis, which involved direct sequencing, MLPA analysis, quantitative PCR of *PAX3,* and analysis of the predicted 3D structure of PAX3. The normal-hearing control group comprised 92 subjects who had normal hearing according to pure tone audiometry. *Results:* In one family, direct sequencing of *PAX3* identified a heterozygous mutation, p. I59F. Analysis of PAX3 3D structures indicated that this mutation distorted the DNA-binding site of PAX3. In the other family, MLPA analysis and subsequent quantitative PCR detected a large, heterozygous deletion spanning 1759–2554 kb that eliminated 12–18 genes including a whole *PAX3* gene.

Keywords: *Mutation, MLPA, clinical diagnosis, hearing loss, dystopia canthorum, pigmentary disorder*

Introduction

Waardenburg syndrome (WS) is a hereditary auditory pigmentary disorder that is responsible for 1–3% of congenital deafness cases [1]. WS is classified into four types based on symptoms other than the auditory and pigmentary disorder. Type I WS (WS1) includes dystopia canthorum, and this feature distinguishes WS1 from type II WS. Type III WS is similar to WS1 but is associated with musculoskeletal anomalies of the upper limbs. Type IV WS is similar to type I but is associated with Hirschsprung disease. Diagnostic criteria for WS1 have been proposed [2]. The clinical features of WS1 demonstrate incomplete penetrance and highly varied expression [3,4], which makes diagnosis in individual patients challenging. For example, WS1 patients may present only one isolated symptom. Diagnosis of high nasal root and medial eyebrow flare can be difficult when they are mild. Hearing loss and early graying are relatively common in the general population and are not specific to WS1. Thus, the accuracy of WS1 diagnosis needs to be improved by the use of additional diagnostic procedures.

It is reported that more than 90% of patients with WS1 harbor point mutations in *PAX3* [5], and an additional 6% of WS1 patients harbor partial or complete *PAX3* deletions [6]. This high frequency of *PAX3* mutation in WS1 suggests that clinical diagnosis of WS1 could be facilitated by *PAX3* genetic analysis. To date, more than 80 *PAX3*

Correspondence: Tatsuo Matsunaga, Department of Otolaryngology, Laboratory of Auditory Disorders, National Institute of Sensory Organs, National Tokyo Medical Center, 2-5-1 Higashigaoka, Meguro, Tokyo, 152-8902, Japan. Tel: +81 3 3411 0111. Fax: +81 3 3412 9811. E-mail: matsunagatatsuo@kankakuki.go.jp

This study was presented at the annual meeting of the Collegium Oto-Rhino-Laryngologicum Amicitiae Sacrum, Rome, August 28, 2012.

(Received 19 September 2012; accepted 20 October 2012)

ISSN 0001-6489 print/ISSN 1651-2251 online
DOI: 10.3109/00016489.2012.744470

mutations are reported to be associated with WS1 [5]. A de novo paracentric inversion on chromosome 2 in a Japanese child with WS1 provided a clue for identification of *PAX3* in the distal part of chromosome 2 [7]. However, only a few *PAX3* mutations including the chromosomal inversion have been reported in Japanese patients with WS1 since then [8,9].

In the present study, we conducted *PAX3* genetic analysis to facilitate diagnosis of WS1 in two Japanese families. In one family, to verify the pathogenicity of an identified missense mutation, we analyzed the effect of the mutation on the three-dimensional (3D) structure of PAX3. In the other family, no mutations were identified by direct sequencing, so multiple ligation-dependent probe amplification (MLPA) analysis was used to search for large deletions in *PAX3* and thereby increase the sensitivity of genetic diagnosis.

Material and methods

Patients and control subjects

Two Japanese families with WS1 were included in the study. The diagnosis of WS1 was based on criteria proposed by the Waardenburg Consortium [2]. The normal-hearing controls comprised 92 subjects who had normal hearing according to pure tone audiometry. This study was approved by the institutional ethics review board at the National Tokyo Medical Center. Written informed consent was obtained from all subjects included in the study or from their parents.

Clinical evaluation

A comprehensive clinical history was taken from subjects who were examined at our hospitals or from their parents. During physical examination, special attention was given to the color of the skin, hair, and iris, and to other anomalies such as dystopia canthorum, medial eyebrow flare, limb abnormalities, and Hirschsprung disease. After otoscopic examination, behavioral audiometric testing was performed. The test protocol was selected according to the developmental age of the subject (conditioned orientation response audiometry, play audiometry, or conventional audiometric testing, from 125 to 8000 Hz), and testing was performed using a diagnostic audiometer in a soundproof room. Auditory brainstem response (ABR) and otoacoustic emission were also evaluated in some subjects.

Direct sequencing

Genomic DNA from the subjects was extracted from peripheral blood leukocytes using the Gentra Puregene® Blood kit (QIAGEN, Hamburg, Germany). Mutation screening of *PAX3* was performed by bidirectional sequencing of each exon (exons 1–11) together with the flanking intronic regions using an ABI 3730 Genetic Analyzer (Applied Biosystems, Foster City, CA, USA). Primer sequences for *PAX3* are listed in Table I. Mutation nomenclature is based on the genomic DNA sequence of [GenBank accession no. NG_011632.1], with the A of the translation initiation codon considered as +1. Nucleotide conservation between mammalian species was evaluated using ClustalW (http://www.ebi.ac.uk/Tools/msa/clustalw2/). PolyPhen-2 software (http://genetics.bwh.harvard.edu/pph2/) was used to predict the functional consequence(s) of each amino acid substitution.

MLPA

MLPA analysis was performed using an MLPA kit targeting *PAX3*, *MITF*, and *SOX10* (SALSA MLPA Kit P186-B1, MRC-Holland, Amsterdam, The Netherlands) according to the manufacturer's protocol. Exon-specific MLPA probes for exons 1–9 of *PAX3* and control probes were hybridized to genomic DNA from the subjects and normal controls and ligated with fluorescently labeled primers. A PCR reaction was then performed to amplify the hybridized probes. The amplified probes were fractionated on an ABI3130xl Genetic Analyzer (Applied Biosystems) and the peak patterns were evaluated using GeneMapper (Applied Biosystems).

Real-time PCR

To determine the length of each deleted genomic region, 100 ng of genomic DNA from the subjects and a normal control were subjected to quantitative PCR (Prism 7000, Applied Biosystems) using Power SYBR® Green Master Mix (Life Technologies, Carlsbad, CA, USA) and 12 sets of primers designed to amplify sequence-tagged sites on chromosome 2 (GenBank accession nos: RH46518, RH30035, RH66441, GDB603632, 1988, RH24952, RH47422, RH65573, RH26526, RH35885, RH16314, and RH92249).

Homology modeling of the PAX3 paired domain

The DNA-binding site of the paired domain of PAX3 was modeled using SWISS-MODEL [10] with the crystal structure of the PAX5 paired domain-DNA complex (PDB ID:1PDN_chain C) as the template because PAX3 and PAX5 are functionally and structurally similar [11]. The amino acid

Table I. Primer sequences for *PAX3*.

Exon 1	Forward	5′-TGTAAAACGACGGCCAGTAGAGCAGCGCGCTCCATTTG-3′
	Reverse	5′-CAGGAAACAGCTATGACCGCTCGCCGTGGCTCTCTGA-3′
Exon 2	Forward	5′-TGTAAAACGACGGCCAGTAAGAAGTGTCCAGGGCGCGT-3′
	Reverse	5′-CAGGAAACAGCTATGACCGGTCTGGGTCTGGGAGTCCG-3′
Exon 3	Forward	5′-TGTAAAACGACGGCCAGTTAAACGCTCTGCCTCCGCCT-3′
	Reverse	5′-CAGGAAACAGCTATGACCGGGATGTGTTCTGGTCTGCCC-3′
Exon 4	Forward	5′-TGTAAAACGACGGCCAGTAATGGCAACAGAGTGAGAGCTTCC-3′
	Reverse	5′-CAGGAAACAGCTATGACCAGGAGACACCCGCGAGCAGT-3′
Exon 5	Forward	5′-TGTAAAACGACGGCCAGTGGTGCCAGCACTCTAAGAACCCA-3′
	Reverse	5′-CAGGAAACAGCTATGACCGGTGATCTGACGGCAGCCAA-3′
Exon 6	Forward	5′-TGTAAAACGACGGCCAGTTGCATCCCTAGTAAAGGGCCA-3′
	Reverse	5′-CAGGAAACAGCTATGACCGGTGTCCATGGAAGACATTGGG-3′
Exon 7	Forward	5′-AACTATTATTTCATCAGTGAAATC-3′
	Reverse	5′-ATTCACTTGTATAAAATATCCACC-3′
Exon 8	Forward	5′-TGTAAAACGACGGCCAGTTGAAGCCAGTAGGAAGGGTGGA-3′
	Reverse	5′-CAGGAAACAGCTATGACCTGCAGGTTAAGAAACGCAGTTTGA-3′
Exon 9a	Forward	5′-TGTAAAACGACGGCCAGTTTGATACCGGCATGTGTGGC-3′
	Reverse	5′-CAGGAAACAGCTATGACCTGCAGTCAGATGTTATCGTCGGG-3′
Exon 9b	Forward	5′-TGTAAAACGACGGCCAGTCACAACTTTGTGTCCCTGGGATT-3′
	Reverse	5′-CAGGAAACAGCTATGACCGGGACTCCTGACCAACCACG-3′
Exon 10–11	Forward	5′-TGTAAAACGACGGCCAGTGCAAATGGAATGTTCTAGCTCCTCG-3′
	Reverse	5′-CAGGAAACAGCTATGACCGGTCAGCTCCAGGATCATATGGG-3′

sequences of the PAX3 and PAX5 paired domains were 79% homologous. The predicted PAX3 structure and the p.I59F mutation structure were superimposed on the backbone atoms of the PAX5 paired domain-DNA complex and displayed using the extensible visualization system, UCSF Chimera [12].

Results

In family 1, the proband, a 9-month-old male, was the first child of unrelated Japanese parents. Abnormal responses were found upon newborn hearing screening in the left ear, and left hearing loss was diagnosed by ABR. On physical examination, dystopia canthorum was noted, with a W-index of 2.77. The patient's mother also had dystopia canthorum, with a W-index of 2.68. She also had a history of early graying that started at age 16 years. She had not been diagnosed with WS1. According to the parents, 10 members of this family, including the proband and the mother, showed clinical features consistent with WS1 (Figure 1). ABR performed in the proband

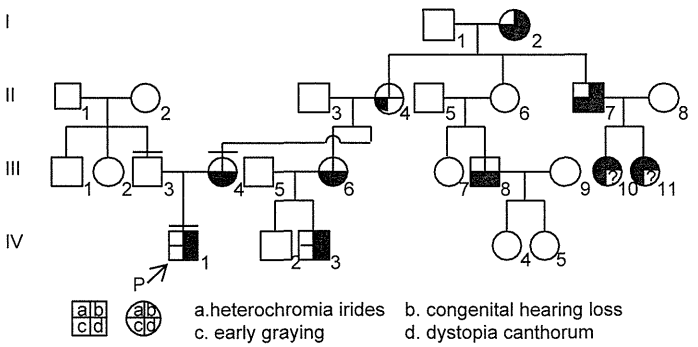

Figure 1. Pedigree of family 1. The proband is indicated by an arrow. The individuals we examined personally are indicated by a bar over the symbol. Phenotypes observed in this family are indicated symbolically as detailed below the pedigree.

revealed normal hearing in the right ear and no responses to 105 dB click stimuli in the left ear. Computed tomography (CT) of the temporal bone showed normal structures in the inner, middle, and outer ears.

Genetic analysis of *PAX3* was conducted in this family, and direct sequencing of *PAX3* revealed a heterozygous mutation, c.175A>T, in the proband and his mother. This mutation resulted in a missense mutation, p.I59F (Figure 2A). The proband's father did not harbor this mutation. p.I59F is located within exon 2 and is part of the paired domain of *PAX3*, which is a critical region for interaction between transcription factors and target DNA (Figure 2B). A multiple alignment of *PAX3* orthologs at this region demonstrated that I59 was evolutionarily conserved among various species (Figure 2C). The p.I59F mutation was not identified in any of the 184 alleles from the normal control subjects. This mutation was predicted to be 'probably damaging' according to PolyPhen-2 software.

The predicted 3D structures of the paired domain of the PAX3-DNA complex indicated that the PAX3 paired domain binds to the corresponding DNA (white double helixes) via hydrogen bonds (pink lines) at the N-terminal of α-helix1 (H1), α-helix2 (H2), and α-helix3 (H3) (indicated in blue; Figure 3A). I59 is located in the middle of H1, H2, and H3 and is surrounded by hydrophobic residues (green) protruding from H1, H2, and H3. Because the van der Waals radius of phenylalanine (Figure 3C; white arrows) is larger than that of isoleucine (Figure 3B, white arrowheads), F59 repels the surrounding hydrophobic residues by van der Waals forces and increases the distance between F59 and the surrounding hydrophobic residues, resulting in structural distortion of the DNA-binding site of PAX3. Since this site is precisely shaped for maximal binding to the corresponding DNA, this mutation is likely to reduce the binding ability of the paired domain of PAX3 and cause WSI. A mutational search found the same mutation in another Japanese family [8].

In family 2, the proband, a female aged 4 years and 4 months, was the first child of unrelated Japanese parents. Abnormal responses were found upon newborn hearing screening in the right ear, and right hearing loss was diagnosed by ABR. On physical examination, dystopia canthorum, medial eyebrow flare, and a white forelock were noted. She was admitted to hospital suffering from ketotic hypoglycemia of unknown cause when aged 4 years. Her mother presented with heterochromia iridis, dystopia canthorum, and medial eyebrow flare, and her grandmother presented with early graying that started at around 20 years of age, dystopia canthorum, and

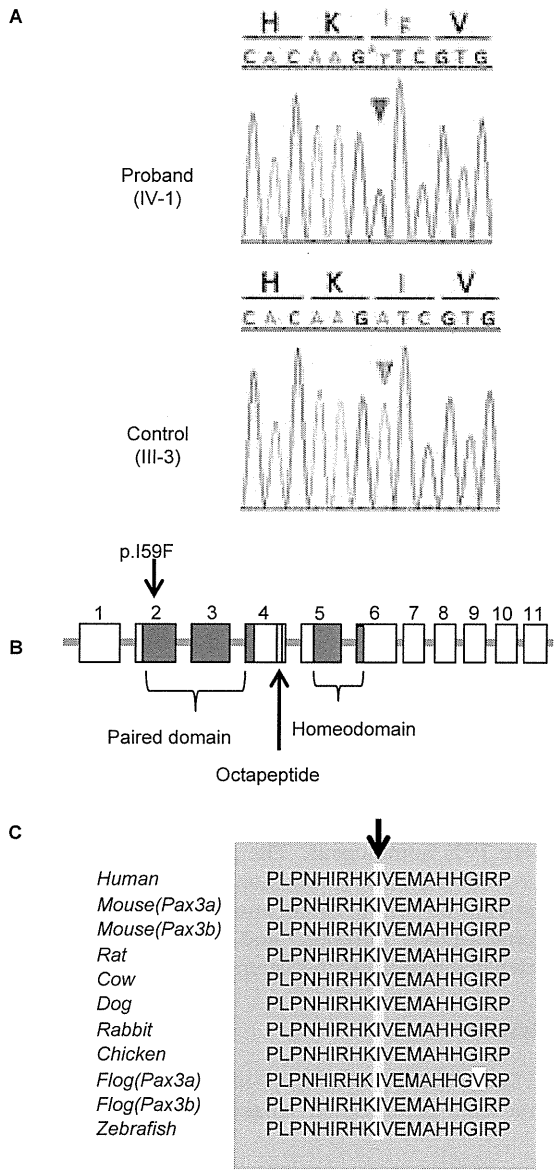

Figure 2. The p.I59F mutation of *PAX3* detected in family 1. (A) Sequence chromatogram for the proband and unaffected control. A heterozygous A to T transversion (red arrowhead) that changes codon 59 from ATC, encoding isoleucine (I), to TTC, encoding phenylalanine (F), was detected in the proband but not in the control (green arrowhead). (B) Localization of the p.I59F mutation and functional domains of PAX3. (C) A multiple alignment of PAX3 orthologs. Regions of amino acid sequence identity are shaded gray. The position of I59 is indicated by an arrow and shaded yellow.

medial eyebrow flare. According to the grandmother, the father of the grandmother also had dystopia canthorum and medial eyebrow flare. The pedigree of family 2 is shown in Figure 4. The grandmother

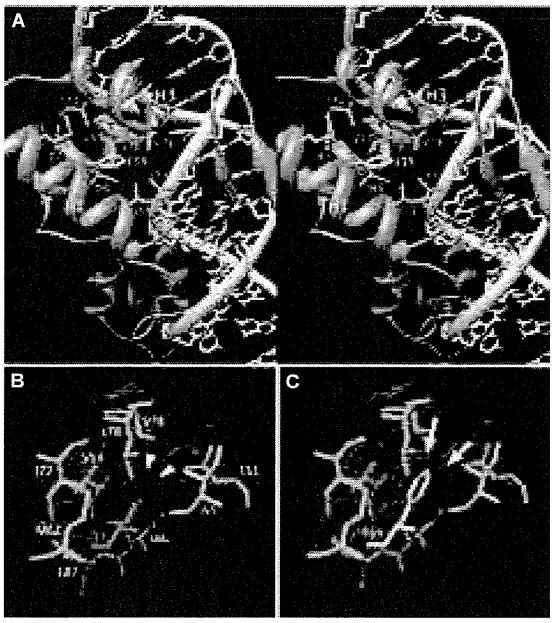

Figure 3. The predicted structure of the PAX3 paired domain-DNA complex. (A) The stereo view indicates that the mutated residue was surrounded by hydrophobic residues (green) protruding from H1, H2, and H3 of the paired domain (blue), which binds to DNA (white, sugar; blue, nitrogen; red, oxygen). The pink lines indicate hydrogen bonds. Magenta and yellow residues indicate I59 and F59, respectively. (B, C) The colored spheres indicate the van der Waals surface boundaries, the radius of the hydrophobic residues is shown in green, I59 is shown in magenta and is also indicated by arrowheads, and F59 is shown in yellow and is also indicated by arrows.

and her father had never been diagnosed with WS1. Pure tone audiometry of the proband showed severe hearing loss in the right ear and normal hearing in the left ear. The results of ABR and distortion product otoacoustic emissions in the proband were compatible with those obtained for pure tone audiometry.

Because direct sequencing of *PAX3* in the proband and her grandmother revealed no mutations, we conducted MLPA analysis to search for a large deletion of *PAX3*, and found that the copy number of all tested exons (exons 1–9) of *PAX3* was half that of the number of other chromosomal regions in both subjects (Figure 5A). In control subjects, all tested exons of *PAX3* showed the same copy number as the other chromosomal regions (Figure 5B). To determine the size of the deleted region, quantitative PCR was performed at 12 sequence-tagged sites on chromosome 2q36, which includes *PAX3*. In the proband, copy numbers at nine sites in the middle of the tested region (white arrows) were half that of those examined in normal controls, but the copy numbers at three of the sites near the 5' and 3' ends of the tested region (black arrows) were identical to those examined in normal controls (Figure 6). This result demonstrated that the chromosomal region spanning 1759–2554 kb at 2q36, which includes the whole *PAX3* gene, was deleted in one of the alleles of the proband. The same results were detected in the grandmother. A search for the deleted region revealed that this region contained between 12 and 18 genes, including *PAX3*.

Discussion

The heterozygous missense mutation, p.I59F, was identified in family 1. The pathogenicity of a novel or rare missense mutation in the causative gene is not necessarily verified even when the mutation is absent from a large number of normal controls, when the residue is evolutionary conserved among different species, or if the mutation is associated with the phenotype within a family, because an identified

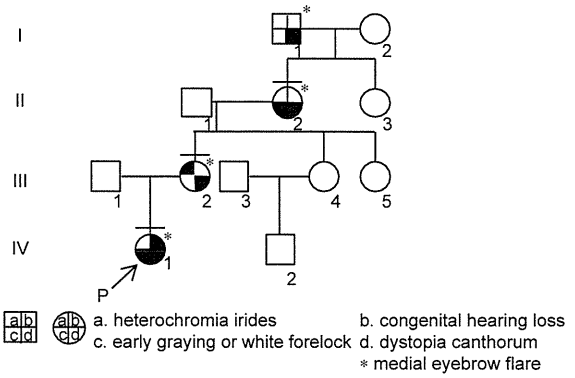

Figure 4. Pedigree of family 2. The proband is indicated by an arrow. The individuals we examined personally are indicated by a bar over the symbol. Phenotypes observed in this family are indicated symbolically, as detailed below the pedigree.